membranes

MDPI

Article

Optimisation of Key Parameters for the Pretreatment Stage of Anion Exchange Membranes in Water Electrolysis

Manuel Ángel González [1,*], Francisca Segura [1], José Manuel Andújar [1] and Concepción Valencia [2]

[1] Research Centre on Technology, Energy and Sustainability (CITES), University of Huelva, 21071 Huelva, Spain; francisca.segura@diesia.uhu.es (F.S.)
[2] Chemical Product and Process Technology Research Centre (Pro2TecS), University of Huelva, 21071 Huelva, Spain
* Correspondence: manuelangel.gonzalez@diesia.uhu.es

Abstract

This research identifies the key parameters influencing the pretreatment stage of anion exchange membranes (AEMs). Using linear sweep voltammetry (LSV), chronopotentiometry, and physicochemical characterisation techniques (ATR-FTIR and swelling ratio), it systematically evaluates the effects of different cleaning protocols, number and duration of immersion steps, electrolyte concentration and type, and physicochemical properties of AEMs on the pretreatment stage. The findings demonstrate that optimal AEM performance during pretreatment is achieved by combining membranes with suitable physicochemical properties (specific conductivity > 25 mS·cm^{-1}, ion exchange capacity > 2.0 meq·g^{-1}, and thickness in the range of 20–30 µm) with optimised alkaline medium conditions (0.1 M KOH for 24 h). The combination of these parameters increase the Faradaic efficiency by 8.8% and the current density during water electrolysis (397.77 ± 14.85) mA·cm^{-2} at 2.3 V, compared with non-pretreated membranes (135.00 ± 33.97) mA·cm^{-2}, membranes that do not exhibit optimal physicochemical properties (323.16 ± 2.56) mA·cm^{-2} and membranes pretreated using inadequate pretreatment parameters (329.08 ± 12.16) mA·cm^{-2}. In addition, membranes pretreated with Milli-Q water for 24 h followed by in-cell conditioning yield comparable performance (391.01 ± 4.11) mA·cm^{-2} at 2.3 V, reducing reagent consumption. The reagent-free pretreatment protocol was validated in a four-cell stack operating for 100 h at 60 °C, achieving a current density of 500 mA·cm^{-2} at 1.91 V per cell using Ni/NiFe as the electrocatalysts.

Keywords: anion exchange membranes; hydrogen production; water electrolysis; pretreatment stage; electrochemical performance

Check for updates

Academic Editor: Vladislav A. Sadykov

Received: 29 October 2026
Revised: 25 November 2026
Accepted: 25 November 2026
Published: 28 November 2026

Copyright: © 2026 by the authors. Licensee MDPI, Basel, Switzerland. This article is an open access article distributed under the terms and conditions of the Creative Commons Attribution (CC BY) license.

1. Introduction

In recent decades, the use of fossil fuels in global energy systems has become a major source of pollution and the principal cause of global warming. Among the alternative fuels available on the market, hydrogen stands out from the rest due to its high energy content (120 kJ·g^{-1}) [1], its ability to be stored for longer periods than electricity, it does not generate toxic gases during combustion and it can be obtained from renewable sources. Green hydrogen, produced through water electrolysis powered by renewable electricity, is gaining increasing attention as a sustainable energy carrier with the potential to contribute to industrial decarbonisation and the transition towards cleaner energy systems [2–4]. Water electrolysis is particularly promising for large-scale hydrogen production because it uses water as a feedstock and enables the production of high-purity hydrogen (>99%).

Among the various water electrolysis technologies currently available on the market, anion exchange membrane water electrolysers (AEMWEs) are the most promising option [5–7]. AEMWE technology uses alkaline solutions like alkaline water electrolysers (AWE), although AEMWE solutions are less concentrated (0.1–1 M KOH). In addition, it is not necessary to use precious metal electrocatalysts and water with a low conductivity, as in the case of proton exchange membrane water electrolysers (PEMWEs) [8–11]. Taking all the advantages of AEMWEs into account, there is a great deal of interest in optimising hydrogen production and improving the performance and lifespan of this electrolysis technology.

To improve the performance of AEMWEs, one of the key points is to ensure the correct hydration and ionic conductivity of AEMs. The general structure of AEMs is formed by a hydrocarbon backbone linked to ammonium groups with different counterions depending on the manufacturer (chloride, bromide, etc.) [12–14]. When the membrane is immersed in an alkaline medium (typically KOH dissolved in water), the water opens the internal channels of the membrane, and the counterions of the ammonium groups are replaced by OH^- ions. Once the internal channels of the membrane have been opened and the exchange of counterions for OH^- ions has occurred during pretreatment, the membrane presents ion exchangeable sites which allow OH^- to migrate during electrolysis. If a good level of hydration is reached, a better diffusivity of OH^- between both sides of the membrane occurs (Figure 1). This entire process is governed by a general transport mechanism based on the vehicular (standard diffusion) and Grotthuss mechanism [15–18].

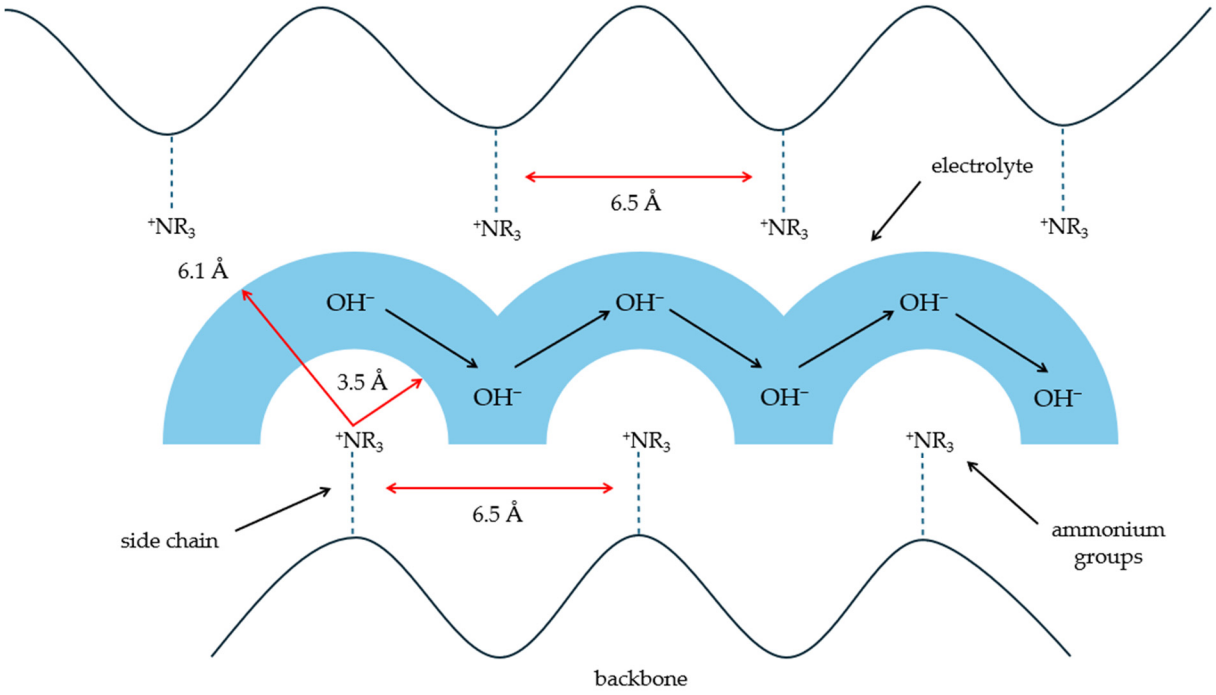


Figure 1. Vehicular and Grotthuss mechanism in the internal channels of AEMs [15].

Before electrolysis, AEMs must be properly pretreated to enhance the hydration and ion exchange process. If AEMs do not exhibit suitable physicochemical properties for the pretreatment stage (specific conductivity, ion exchange capacity, thickness, etc.) or are not pretreated under optimal conditions (time of immersion, concentration, electrolyte, etc.), they are susceptible to swelling and degradation reactions, which adversely affect the electrochemical performance of the system [11,12]. AEMs have a low chemical stability and there are different reaction pathways through which the degradation process takes place. According to several authors, the main reaction pathways are the following: Hoffman elimination, nucleophile substitution (SN2) and ylide intermediate formation [14,19–21].

Given the importance of determining the optimal parameters to favour the hydration and ion exchange process during the pretreatment stage while avoiding excessive swelling and degradation reactions, this study conducts a multi-parametric investigation to identify the parameters that affect the pretreatment stage. Most studies employ generic protocols, do not identify the optimal physicochemical properties that AEMs must have to carry out the pretreatment stage (thickness, specific conductivity, ion exchange capacity, etc.) or they do not justify how different parameters (time of immersion, concentration, electrolyte, etc.) influence the hydration, ion exchange process, swelling, and overall AEMWE performance (Table 1) [22–25].

Most studies focus on other aspects, such as AEMs synthesis, electrocatalysts and ionomers, or porous transport materials [5], Figure 2. Given the limited information available, this study systematically identifies the optimal parameters to carry out the pretreatment in an alkaline medium, including cleaning protocols, number of immersions, time of immersion, electrolyte concentration, type of electrolyte and physicochemical properties of AEMs. In parallel, and drawing upon data from previous studies [26], an alternative aqueous protocol is optimised based on the optimal parameters established through the alkaline methodology.

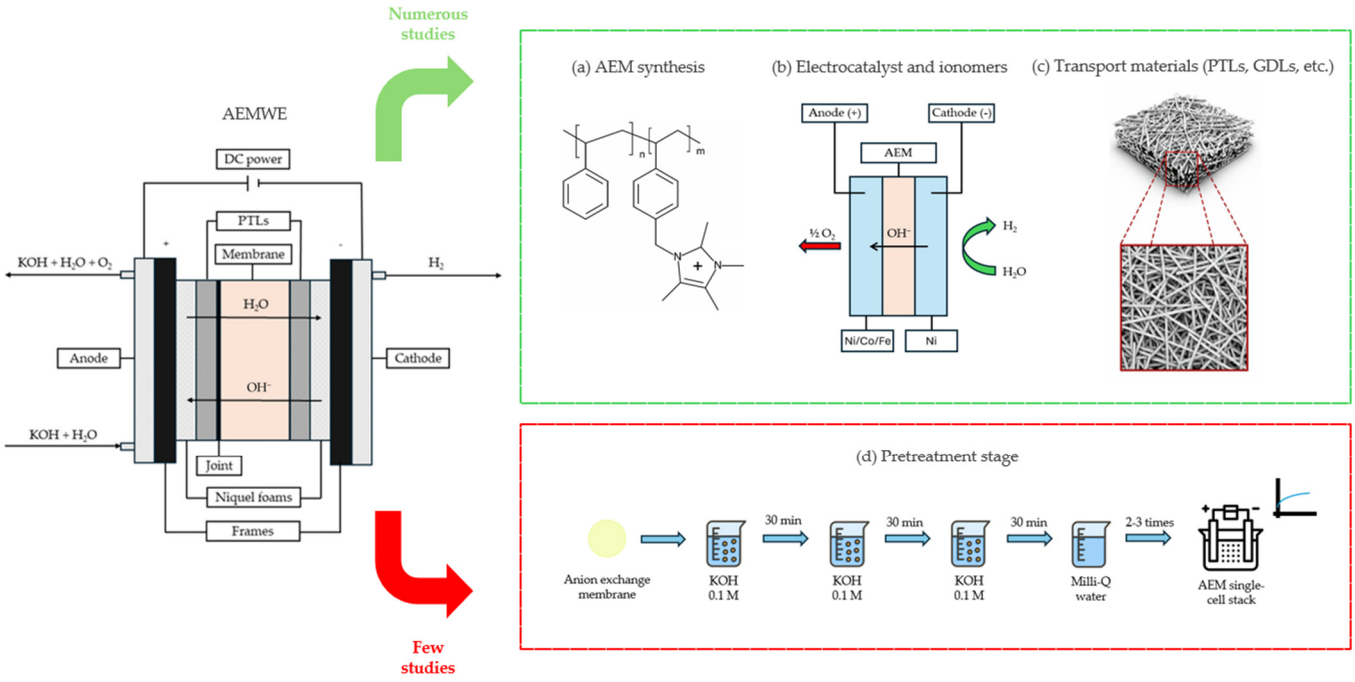


Figure 2. Previous research associated with AEM electrolysis technology: (**a**) AEM synthesis, (**b**) electrocatalyst and ionomers, (**c**) transport materials (PTLs, GDLs, etc.); authors' proposal: (**d**) pretreatment protocols.

Table 1. Authors' contributions and related studies.

Scientific Studies	Key Contributions	Multi-Parametric Study	Characterisation Techniques to Study the Pretreatment Stage
Authors' Proposal	A multi-parametric study is conducted in an alkaline medium, encompassing cleaning protocols, number of immersions, time of immersion, electrolyte concentration, type of electrolyte and the identification of the optimal physicochemical properties of AEMs for the pretreatment stage. Furthermore, an alternative reagent-free pretreatment is proposed.	Several parameters are studied until proper membrane hydration and ion exchange is achieved without degrading the AEM. The results were evaluated by measuring the current density at different cell voltages and through complementary characterisation techniques.	LSVs, chronopotentiometries, ATR-FTIR analysis and swelling ratio measurements

Table 1. *Cont.*

Scientific Studies	Key Contributions	Multi-Parametric Study	Characterisation Techniques to Study the Pretreatment Stage
[22]	The materials and manufacturing process for the state-of-the-art AEM pure water electrolysers were described, which offer cutting-edge performance and durability, although substantial improvements are still needed for commercial relevant performance.	It describes that during electrolyser operation, different electrolyte pretreatments affect the measured performance and durability of the electrolyser, but it does not conduct a study to optimise the pretreatment parameters.	n/a
[23]	Methodology for a comparative analysis of different electrodes regarding their energy demand and material criticality.	AEMs were pretreated with 1.0 M KOH solution and stored in fresh 1.0 M KOH solution, but no justification is given for its selection.	n/a
[24]	Fabrication conditions of membrane electrode assembly (MEA) and working condition of water electrolysis are investigated in detail.	AEMs were pretreated by circulating 200 mL 1.0 M KOH solution through the cell for 4.0 h at 60 °C, but no justification is given for its selection.	n/a
[25]	Two AEMWE models using non-noble metal-based components were developed. Three components of the membrane electrode assembly were examined to be substituted for a non-noble metal.	AEMs were pretreated with a 1 M KOH solution for 1 h and rinsed with deionized water, but no justification is given for its selection.	n/a

2. Materials and Methods

As shown in Table 2, the materials and equipment used by the authors to carry out the research are divided into the following parts: Stage (1) Multi-parametric study of the pretreatment stage and Stage (2) Test bench and characterisation equipment.

Table 2. Materials and equipment used by the authors in the research.

Stages	Materials and Equipment Technical Data
(1) Multi-parametric study of the pretreatment stage	Potassium hydroxide, KOH, Alquera®, p.a = 90% (Madrid, Spain) Sodium hydroxide, NaOH, MP biomedicals, p.a ≥ 97% (Solon, OH, USA) Rubidium hydroxide hydrate, $RbOH{\cdot}H_2O$, Sigma-Aldrich®, Impurities ≤ 15% Rb_2CO_3 (St. Louis, MO, USA) Milli-Q water, HYDROLAB®, ϱ = 18.2 MΩ·cm (Hydrolab Sp. z o.o., Straszyn, Poland) Fumasep® FAA-3-50 membrane, brominated polysulfone backbone with quaternary ammonium side chain groups (FUMATECH BWT GmbH, Bietigheim-Bissingen, Germany) Fumasep® FAD-55 membrane, brominated polysulfone backbone with quaternary ammonium side chain groups (FUMATECH BWT GmbH, Bietigheim-Bissingen, Germany) PiperION® Versogen's membrane, poly(aryl piperidinium) polymer (Versogen, Inc., Wilmington, DE, USA) Tokuyama® A210 membrane, chlorinated hydrocarbon polymer backbone with quaternary ammonium side chain groups (Tokuyama Corporation, Tokyo, Japan)
(2) Electrochemical characterisation	AEM stack (in-house manufacturing), cell active area 63.62 cm^2 Peristaltic pump: Tapflo®—PT10 GR-05/43 (Tapflo AB, Kungälv, Sweden) Power supply: Rate power = 3000 W, Output = 0.1–100 A (Newpower, Shenzhen, China) JASCO FT/IR-4200: Wavenumber range of 4000–500 cm^{-1} (JASCO Corporation, Hachioji, Tokyo, Japan)

2.1. Multi-Parametric Study of the Pretreatment Stage

The parameters studied in this research are summarised in Table 3. To compare the results obtained and to study the degree of hydration, ion exchange and current density, a baseline test (Test #0) has been established. This configuration is based on the authors' previous research [26], and it consists of: circular-shaped AEMWE single-cell with a cell active area of 63.62 cm^2, two PTLs (Porous Transport Layers) of SS 316L without electrocatalyst deposition, two nickel foams with 120 PPI (Pores Per Inch)-porosity and 3 mm-thickness, one carbon cloth between the PTL-foam surface of the cathode, and a Fumasep® FAA-3-50 membrane. The single-cell stack is assembled with a 10 N·m torque.

Table 3. Multi-parametric study proposed by authors: objectives and test conditions.

Test	Objective	Multi-Parametric Study
#0	Baseline	Non-pretreated Fumasep® FAA-3-50 membrane
#1	Cleaning effect	#1.1 Membrane immersed three times in 0.1 M KOH for 30 min each time (generic alkaline protocol [26]). #1.2 Membrane immersed three times in 0.1 M KOH for 30 min each time, followed by rinsing in Milli-Q water for 5 min each time.
#2	Number of immersions and pretreatment time effect	#2.1 Membrane immersed four times in 0.1 M KOH for 20 min each time (total time: 80 min). #2.2 Membrane immersed five times in 0.1 M KOH for 10 min each time (total time: 50 min). #2.3 Membrane immersed in 0.1 M KOH for 24 h. #2.4 Membrane immersed in 0.1 M KOH for 7 days.
#3	KOH concentration effect	#3.1 Membrane immersed 0.5 M KOH. #3.2 Membrane immersed in 1 M KOH. #3.3 Membrane immersed in 5 M KOH.
#4	Physicochemical properties of AEMs	#4.1 Membrane Tokuyama® A210. Manufacturer Tokuyama®. #4.2 Membrane PiperION®. Manufacturer Versogen®. #4.3 Membrane Fumasep® FAD-55. Manufacturer Fumatech BWTGmbH®.
#5	Effect of electrolyte type	#5.1 Electrolyte NaOH.
		#5.2 Electrolyte RbOH.
#6	Study inorganic Electrolyte–membrane relationship	#6.1 Immerse the membrane PiperION® in RbOH. #6.2 Immerse the membrane Fumasep® FAD-55 in RbOH.
#7	Comparison with zero reagents-based pretreatment protocol and optimisation of the conditioning stage.	#7.1 Immerse the membrane in Milli-Q water for 7 days (reference aqueous protocol [26]).
		#7.2 Immerse the membrane in Milli-Q water during the optimal time determined in the alkaline methodology.

Note. Tests were conducted consecutively, such that once the optimal conditions for Test #i, (i = 1, 2, ..., 6) they were maintained in Test #i + 1, and so on. Test #7 corresponds to the aqueous protocols. New membrane is used in each Test #i.j, (j = 1, 2, ..., 4).

The Fumasep® FAA-3-50 membrane has been chosen as a starting point, and from this baseline, the best parameters of each test will be identified, and the optimal conditions will be maintained to continue the research. A new membrane was used for each test to ensure the reliability of the results and prevent cross-contamination.

2.2. Electrochemical Characterisation

For the experimental tests, an AEMWE single-cell stack and a test bench designed by the authors (Figure 3) have been used. The electrochemical performance of the pretreated

membranes is evaluated based on current density values (mA·cm^{-2}) obtained from the linear sweep voltammetry (LSV) curves on the voltage range 1.4 V–2.5 V.

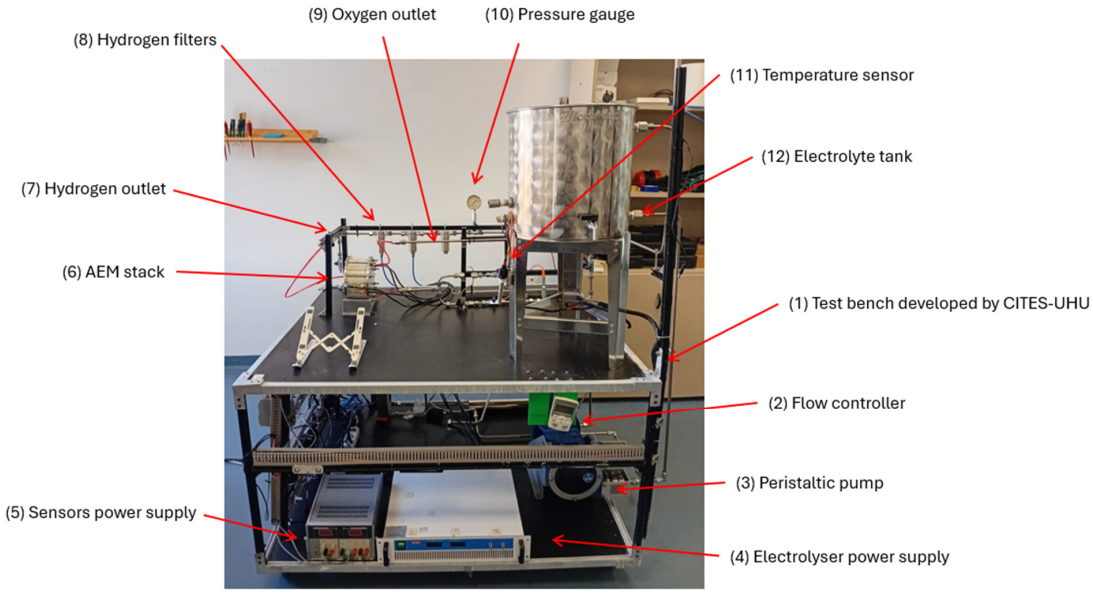


Figure 3. Test bench developed by the authors for testing AEMWE stacks.

For Tests #1 to #6 (alkaline medium), the membranes were activated before operation. For activation, membrane is inserted on the stack, the electrolyte is recirculated (1 M KOH at 25 °C) and a low voltage is applied (1.8 V) until a nominal operating point is reached [26]. For Test #7 (aqueous medium), membrane must be conditioned prior to be activated. Ion exchange to OH^- groups occurs during this stage and not during pretreatment, where the membrane is only hydrated. During the conditioning stage, the electrolyte is recirculating through the AEMWE single-cell stack without applying an external current, whereas during the activation stage, the electrolyte is recirculating while a small voltage is applied to the stack (1.8 V), allowing the membrane to begin operating and reach its nominal activation point. Once both stages are completed, the LSV curves can be recorded. The experimental procedure is outlined as follows:

1. Membrane pretreatment according to data summarised in Table 3.
2. Assembly of the AEMWE single-cell stack.
3. Membrane conditioning (only for aqueous medium, Test #7) inside the AEMWE single-cell stack with 0.1 LPM electrolyte recirculation (1 M KOH at 25 °C) without applying electric current. Conditioning for 8 h [26] in Test #7.1 and conditioning for the optimal time determined by the alkaline methodology in Test #7.2.
4. Membrane activation for 30 min inside the AEMWE single-cell stack with 0.1 LPM electrolyte recirculation (1 M KOH at 25 °C) and electrical supply at 1.8 V.
5. Measurement of three LSV curves by varying the supply voltage from 1.4 V to 2.5 V at 10 min intervals (LSV 1, LSV 2, and LSV 3).
6. Electrolyte recirculation and power supply cut-off for 10 min.
7. Measurement of three LSV curves by varying the supply voltage from 1.4 V to 2.5 V at 10 min intervals (LSV 4, LSV 5 and LSV 6).
8. Electrolyte recirculation and power supply cut-off (end of the test).

The second objective is to analyse the behaviour of the AEMWE single-cell stack over medium periods of operation. For this purpose, chronopotentiometry is used to study the electrochemical performance of the AEMWE. The membranes are subjected to a constant current of 20 A (corresponding to 314.4 mA·cm^{-2}) for 24 h to study the changes in the

voltage value over time. As with the LSV curves, AEMs pretreated in an alkaline medium must be activated, whereas those pretreated in aqueous medium undergo both conditioning and activation.

1. Membrane pretreatment according to data summarised in Table 3.
2. Assembly of the AEMWE single-cell stack.
3. Membrane conditioning (only for aqueous medium, Test #7) inside the AEMWE single-cell stack with 0.1 LPM electrolyte recirculation (1 M KOH at 25 °C) without applying electric current. Conditioning for 8 h [26] in Test #7.1 and conditioning for the optimal time determined by the alkaline methodology in Test #7.2.
4. Membrane activation for 30 min inside the AEMWE single-cell stack with 0.1 LPM electrolyte recirculation (1 M KOH at 25 °C) at constant current of 20 A (314.4 mA·cm^{-2}).
5. Chronopotentiometry test for 24 h at constant current of 20 A (314.4 mA·cm^{-2}).
6. Electrolyte recirculation and power supply cut-off after 24 h (end of the test).
7. Repeat chronopotentiometry test at 32.5 A (500 mA·cm^{-2}), scaling the stack up to four cells, operating at 60 °C to validate the results under real operating conditions with on/off cycles.

Additionally, ATR-FTIR analysis and swelling ratio (SR) measurements were carried out to validate the results obtained from the LSV and chronopotentiometry tests.

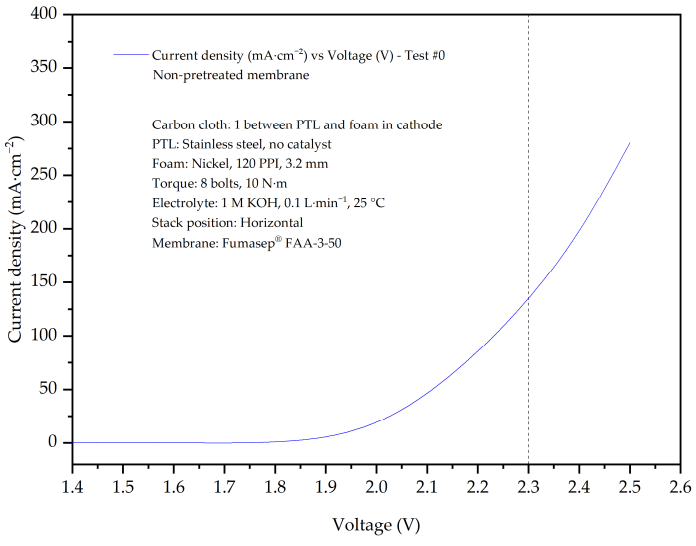
3. Results and Discussion

This section presents the experimental results obtained from the multi-parametric study, together with the results of the LSV, chronopotentiometry, ATR-FTIR and SR analyses.

3.1. Experimental Results from the Multi-Parametric Study

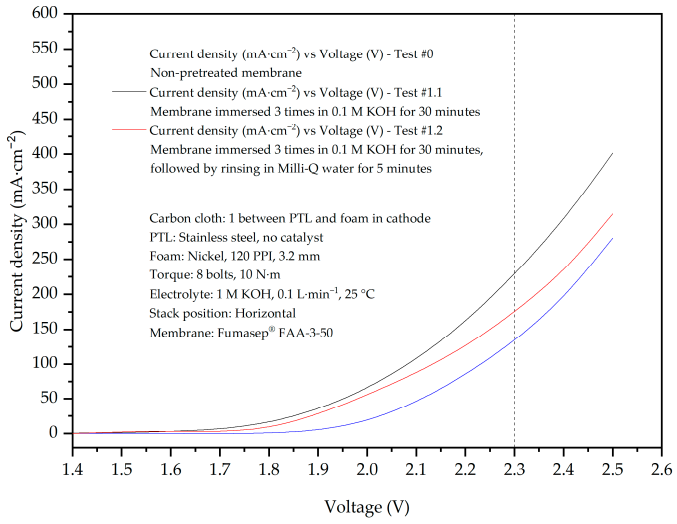
3.1.1. Test #0. Baseline

The LSV curves show low current densities (Figure 4a), indicating that the Fumasep® FAA-3-50 membrane has not achieved a sufficient degree of hydration and ion exchange [27–29]. In addition, membrane hydration under confined conditions (inside the AEMWE stack) limits its swelling capacity, potentially leading to mechanical deterioration of the membrane structure and reducing its service life [30,31].

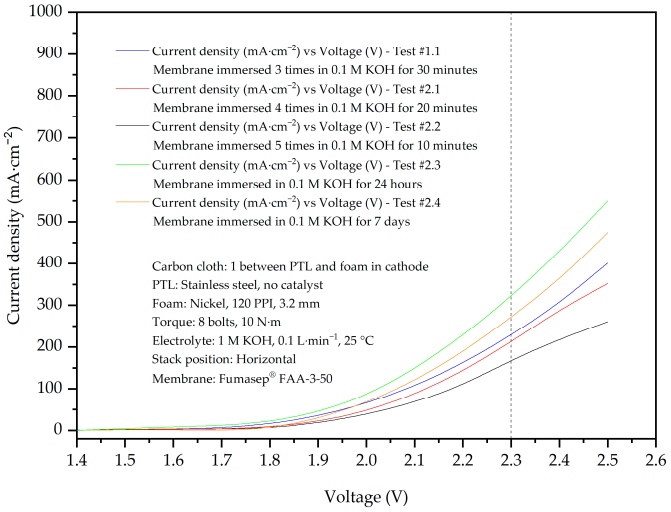


(a)

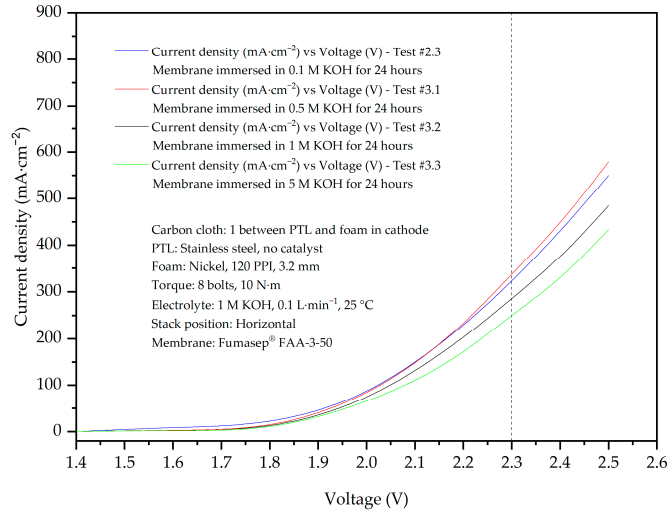
Figure 4. *Cont.*



(**b**)

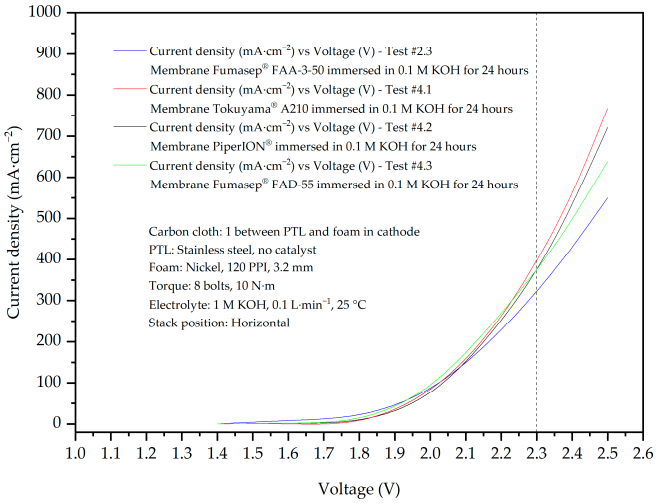


(**c**)

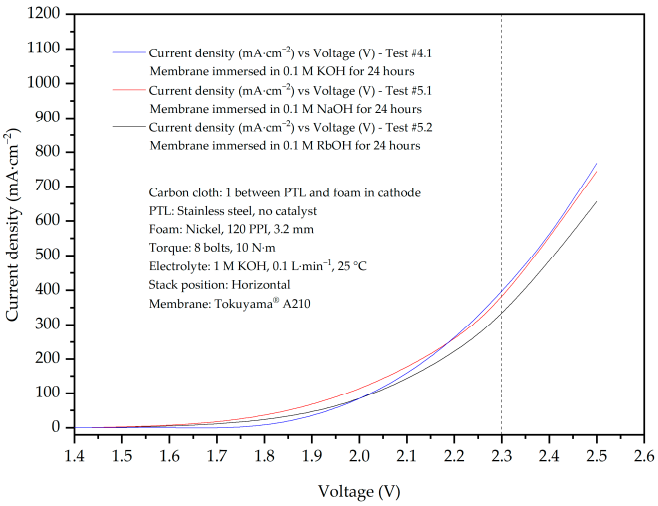


(**d**)

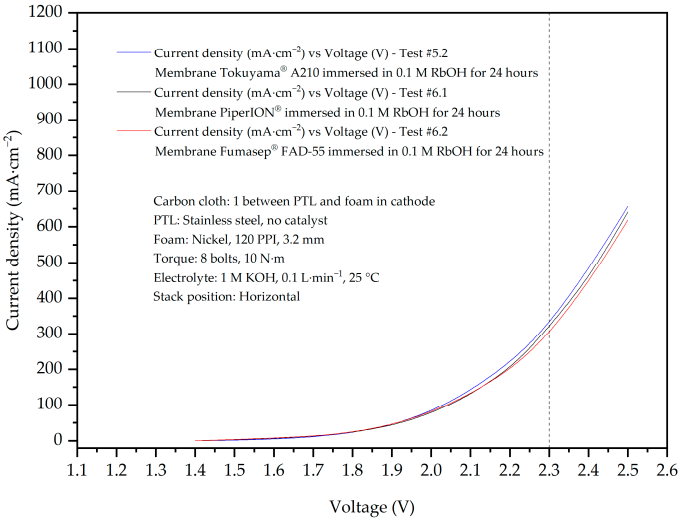
Figure 4. *Cont.*



(**e**)

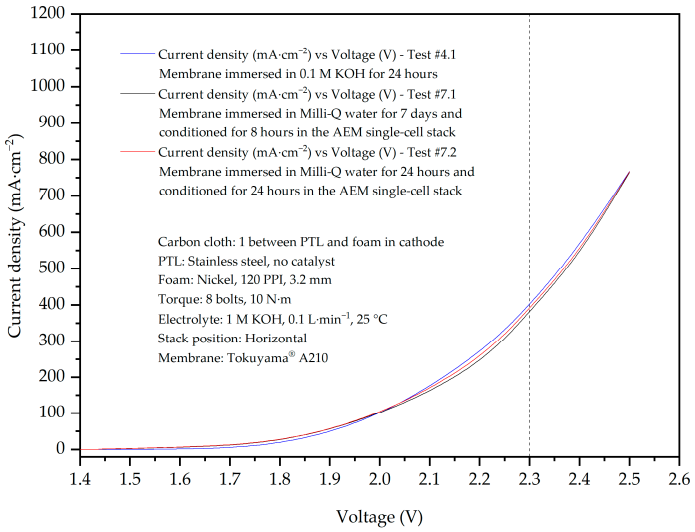


(**f**)



(**g**)

Figure 4. *Cont.*



(**h**)

Figure 4. Current density (mA·cm^{-2}) vs. Voltage (V) after pretreatment protocols. (**a**) Test #0: Non-pretreated Fumasep® FAA-3-50 membrane. (**b**) Test #1: Cleaning protocol. (**c**) Test #2: Number and time of immersion protocol. (**d**) Test #3: KOH concentrations. (**e**) Test #4: Types of membranes. (**f**) Test #5: Type of electrolyte. (**g**) Test #6: Electrolyte–membrane relationship. (**h**). Test #7: Zero reagent comparison.

Table 4 reports the results obtained from Test #0 (baseline), at nominal cell voltage of 2.3 V. This voltage was selected as a reference for comparison because it is slightly higher than the thermoneutral voltage of the electrolysis reaction (1.48 V under typical conditions). This allows the reaction to proceed at practical current densities without requiring excessively high voltages, which would increase energy losses, degradation and parasitic reactions.

Table 4. Baseline Test #0. Current density (mA·cm^{-2}) obtained at 2.3 V for the non-pretreated Fumasep® FAA-3-50 membrane.

Protocol	Cell Voltage (V)	Current Density (mA·cm^{-2})	SD of Current Density (mA·cm^{-2})
Test #0	2.3	135.00	33.97

Note. SD represents the standard deviation of current density (samples number; $n = 6$).

3.1.2. Test #1. Cleaning Protocols

Membrane Fumasep® FAA-3-50 has been immersed in three 0.1 M KOH solutions for 90 min (30 min in each solution) in Test #1.1, while in Test #1.2 the membrane was pretreated following the same protocol as in Test #1.1, but it was cleaned with Milli-Q water for 5 min each time. When analysing the LSV curves (Figure 4b), it is observed that, in both cases, the current density increases compared to Test #0. However, cleaning the membrane with Milli-Q water resulted in a lower current density compared to the membrane that was not subjected to the cleaning process, Table 5. Cleaning the membrane with Milli-Q water removes K^+ ions from its surface, resulting in lower electrochemical performance. This is consistent with previous studies showing that a higher ionic charge at the membrane surface can contribute to increased current densities compared with membranes that have not yet undergone ion loading [32,33].

Table 5. Current density ($mA \cdot cm^{-2}$) obtained at 2.3 V using different cleaning protocols. Test #0: Do not pretreat the membrane externally. Test #1.1: Immerse the membrane three times in 0.1 M KOH for 30 min. Test #1.2: Immerse the membrane three times in 0.1 M KOH for 30 min and clean in Milli-Q water for 5 min.

Protocol	Cell Voltage (V)	Current Density ($mA \cdot cm^{-2}$)	SD of Current Density ($mA \cdot cm^{-2}$)
Test #0	2.3	135.00	33.97
Test #1.1	2.3	229.58	6.99
Test #1.2	2.3	175.87	34.11

3.1.3. Test #2. Number of Immersions and Pretreatment Time

Considering that using the parameters of Test #1.1 (pretreatment with 0.1 M KOH without cleaning with Milli-Q water, with three immersions and 90 min in total) the current density increases, Test #2 studies how the number of immersions and pretreatment times affect the ion exchange process. Tests #2.1 and #2.2 increase the number of immersions to four and five, respectively, and the pretreatment time was reduced to 80 and 50 min, in each case). Therefore, it is not feasible to reduce the pretreatment time by increasing the number of immersions, because the same degree of hydration and ion substitution has not been achieved.

Due to the significant effect of time, it is necessary to determine the optimal time to enhance hydration and ion exchange process. For this reason, Tests #2.3 and #2.4 were conducted, pretreating the membrane for 24 h and 7 days, respectively. As shown in Table 6 and Figure 4c, the membrane pretreated for 24 h (Test #2.3) generates higher current densities than the membrane pretreated for 7 days (Test #2.4). This is due to the degradation of the membrane's polymer chain after being immersed in an alkaline medium for such an extended period [19–21]. For this reason, carrying out the pretreatment for 24 h with 0.1 M KOH is enough to ensure that the membrane reaches a good degree of hydration and that ion exchange takes place, while preventing degradation over long periods of time.

Table 6. Current density ($mA \cdot cm^{-2}$) obtained at 2.3 V using different immersion times. Test #1.1: Immersion three times for 30 min. Test #2.1: Immersion four times for 20 min. Test #2.2: Immersion five times for 10 min. Test #2.3: Immersion one time for 24 h. Test #2.4: Immersion one time for 7 days.

Protocol	Cell Voltage (V)	Current Density ($mA \cdot cm^{-2}$)	SD of Current Density ($mA \cdot cm^{-2}$)
Test #1.1	2.3	229.58	6.99
Test #2.1	2.3	213.23	10.88
Test #2.2	2.3	166.83	7.79
Test #2.3	2.3	323.16	2.56
Test #2.4	2.3	272.46	5.35

3.1.4. Test #3. Electrolyte Concentrations

Once the optimal number of immersions and pretreatment time have been established (Test #2.3, one immersion for 24 h), Test #3 was carried out to analyse the effect of electrolyte concentration on the ion exchange process. Up to this point, a 0.1 M KOH solution has been used, so the experiment was repeated for 24 h, but with a higher concentration of KOH (0.5 M). As shown in Figure 4d, the current density obtained in Test #3.1 (0.5 M KOH) is comparable to Test #2.3 (0.1 M KOH) due to no statistically significant difference was observed between both current density values (Table 7), so the concentration of the electrolyte was further increased to observe some significant effect.

Table 7. Current density ($mA \cdot cm^{-2}$) obtained at 2.3 V using different KOH concentrations. Test #2.3: 0.1 M KOH for 24 h. Test #3.1: 0.5 M KOH for 24 h. Test #3.2: 1 M KOH for 24 h. Test #3.3: 5 M KOH for 24 h.

Protocol	Cell Voltage (V)	Current Density ($mA \cdot cm^{-2}$)	SD of Current Density ($mA \cdot cm^{-2}$)
Test #2.3	2.3	323.16	2.56
Test #3.1	2.3	337.17	12.94
Test #3.2	2.3	285.56	5.48
Test #3.3	2.3	249.77	5.21

When the KOH concentration was raised to 1 M (Test #3.2) and 5 M (Test #3.3), a decrease in current density was also observed. By consulting different sources [34–38], it can be observed that several studies use alkaline solutions with a concentration of 0.1 M KOH to carry out pretreatment. Therefore, this validates the results and confirms that it is not appropriate to use concentrations above or below this value, due to the degradation experienced by the membrane at high concentrations (>0.5 M KOH), and to the low ion exchange capacity at low concentrations (<0.1 M KOH). Since the current densities obtained using 0.1 M and 0.5 M KOH are very similar (Table 7), 0.1 M KOH was chosen as the optimal concentration due to reagent savings and the lower environmental impact of the process. As example, 5.61 g of KOH are required to prepare 1 L of 0.1 M KOH, whereas 28.06 g of KOH are needed to prepare a 0.5 M KOH solution.

3.1.5. Test #4. Physicochemical Properties of the Membrane

After studying the effect of the electrolyte concentration, Test #4 was carried out to determine the optimal physicochemical properties that AEMs must have to enhance the degree of hydration and ion exchange during the pretreatment stage. Table 8 summarises the physicochemical parameters of the tested AEMs (Fumasep® FAA-3-50, Fumasep® FAD-55, Tokuyama® A210 and PiperION®). The selected membranes exhibit favourable physicochemical properties for the pretreatment stage, as they are commercially available materials with high specific conductivity and a high ion exchange capacity. Their morphology consists of ionic channels in which hydrocarbon chains bearing charged groups facilitate water uptake and ion migration between the two compartments of the electrolyser. Owing to their high conductivity values, these membranes facilitate the uptake of OH^- ions into their structure. Furthermore, their high ion exchange capacity allows the membrane counterions to be rapidly replaced by the OH^- ions, thereby enabling ion exchange to take place and completing the synthetic route to obtain the membrane in its final charged state [12–18].

Table 8. Physical-chemical parameters of the membranes tested in this study [26,39].

Membrane	Thickness (μm)	Specific Conductivity in Cl^- Form ($mS \cdot cm^{-1}$)	Ion Exchange Capacity ($meq \cdot g^{-1}$)	Tensile Strength (MPa)	Elongation at Break (%)
Fumasep® FAA-3-50	45–55	3–8	1.6–2.1	25–40	15–60
Fumasep® FAD-55	50–60	25–30	2.0–2.5	>15	>20
Tokuyama® A210	28	NDA	NDA	21	700
PiperION®	20	57.5	2.35	>30	>20

Table 9 and Figure 4e show the performance of the Tokuyama® A210, PiperION® and Fumasep® FAD-55 membranes (Test #4.1, #4.2 and #4.3). PiperION® and Fumasep® FAD-55 membranes exhibit better electrochemical performance than Fumasep® FAA-3-50 membrane, because they have higher specific conductivity and ion exchange capacity (Table 8). However, at higher voltages, the current density obtained with Fumasep® FAD-55 membrane is slightly lower than with the PiperION® membrane, owing to its thickness.

Table 9. Current density ($mA \cdot cm^{-2}$) obtained at 2.3 V using different membranes pretreated with 0.1 M KOH. Test #2.3: Fumasep® FAA-3-50 membrane. Test #4.1: Tokuyama® A210 membrane. Test #4.2: PiperION® membrane. Test #4.3: Fumasep® FAD-55 membrane.

Protocol	Cell Voltage (V)	Current Density ($mA \cdot cm^{-2}$)	SD of Current Density ($mA \cdot cm^{-2}$)
Test #2.3	2.3	323.16	2.56
Test #4.1	2.3	397.77	14.85
Test #4.2	2.3	375.97	40.11
Test #4.3	2.3	375.76	58.03

The PiperION® membrane is particularly noteworthy, it is thinner and it facilitates the hydration and ion exchange process during the pretreatment and, subsequently, the migration of ions during the electrolysis. However, membranes with a low thickness have worse mechanical properties (Table 8) [40,41].

For this reason, the Tokuyama® A210 membrane was selected for further study instead of PiperION® or Fumasep® FAD-55 membranes. The Tokuyama® A210 membrane has an optimal combination of physicochemical properties that favour the pretreatment and electrolysis process.

Table 9 shows the current density values at a voltage of 2.3 V obtained from each membrane, pretreated with KOH 0.1 M for 24 h.

3.1.6. Test #5. Electrolyte Type

From Test #4, the Tokuyama®A210 membrane is selected due to its optimal physicochemical properties and, in Test #5, this membrane is used as baseline to study the effect of different electrolytes (KOH, NaOH and RbOH). In AEMWE, electrolytes derived from inorganic compounds are used due to their good solubility in water. Among inorganic electrolytes, KOH is used instead of NaOH because it is more soluble in water and it has a higher conductivity. K^+ is a larger ion than Na^+, making the compound more soluble in water and allowing the OH^- ions to have greater mobility in the solution (Table 10) [42–45]. Considering this, other inorganic compounds containing larger cations (RbOH), may represent promising alternatives to KOH and NaOH owing to their potentially higher solubility and ionic conductivity.

Table 10. Comparison of chemical properties and relative cost of different electrolytes (NaOH, KOH and RbOH) at 20 °C and 0.1 M [42–45].

Electrolytes	NaOH	KOH	RbOH
Cation size (ppm)	102	138	152
Solubility at 20 °C (g/100 mL)	109	112	180
Conductivity at 20 °C (mS/cm)	21–23	23–25	24–26
Cost (€/g)	0.0459	0.0099	27.00

Regarding Table 11 and Figure 4f, the current density values obtained using KOH (Test #4.1) are slightly higher than those obtained using NaOH (Test #5.1), which is reasonable considering the solubility of the electrolyte and its ionic mobility. However, although a higher current density was expected for RbOH (Test #5.2), given that this electrolyte is more soluble and conductive than KOH and NaOH, the results show the opposite. This behaviour was further examined by comparing the experimental results with previous studies on ion mobility in ion exchange membranes [46,47]. It has been concluded that not only the conductivity, solubility, and cation size can be considered when comparing the effect of the electrolyte.

Table 11. Current density ($mA \cdot cm^{-2}$) obtained at 2.3 V using Tokuyama® A210 membranes pretreated with different electrolytes (0.1 M). Test #4.1: Electrolyte KOH. Test #5.1: Electrolyte NaOH. Test #5.2: Electrolyte RbOH.

Protocol	Cell Voltage (V)	Current Density ($mA \cdot cm^{-2}$)	SD of Current Density ($mA \cdot cm^{-2}$)
Test #4.1	2.3	397.77	14.85
Test #5.1	2.3	374.40	2.27
Test #5.2	2.3	329.08	12.16

According to [46], Rb^+ ions affect the water uptake capacity of the membrane. Although the pretreatment with RbOH is performed at the same concentration as KOH and NaOH, the resulting hydration and ion exchange achieved in the membrane is different, affecting OH^- transport through the polymer matrix. This was also confirmed by chronopotentiometry (Figure 5), which showed a higher voltage (2.3 V) was required to reach the target current density (314.4 $mA \cdot cm^{-2}$), as well as by ATR-FTIR analysis (Figure 6), which showed a lower intensity of the signal in the 4000–3000 cm^{-1} region when RbOH was used. In particular, changes in water uptake and local ion solvation influence membrane swelling, ionic-channel continuity, and overall ion mobility, leading to a lower current density under the same operating voltage [48–51].

On the other hand, the signal associated with the C–N stretching vibration remains unchanged. This indicates that changing the electrolyte does not lead to degradation of the membrane's polymeric backbone. However, differences can be observed in the 1500–1000 cm^{-1} region. This region contains the signal associated with the C–NR_3^+ bond, suggesting degradation of the ammonium groups. Consequently, fewer OH^- exchange sites are available to facilitate ion migration, which explain the lower current density observed during electrolysis.

3.1.7. Test #6. Inorganic Electrolyte–Membrane Relationship

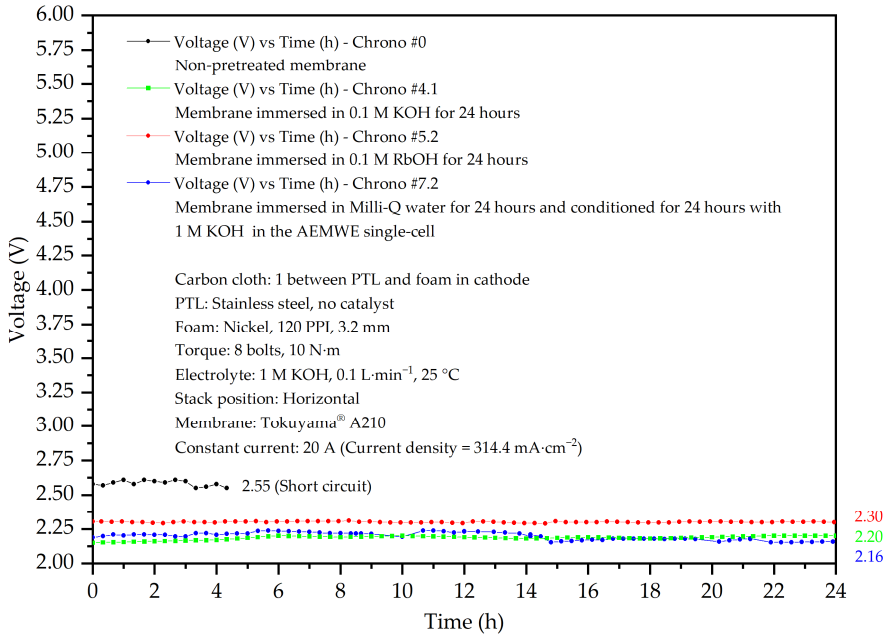
In addition to the previous study, the remaining membranes that exhibited high current densities in Section 3.1.5 (PiperION® and Fumasep® FAD-55) have been tested to verify the effect of RbOH as pretreatment medium. This study was carried out to determine whether the effect generated by the presence of RbOH in the medium affects only the Tokuyama® A210 membrane, or if it exerts a negative effect on other types of membranes. In Table 12, the current density value at a voltage of 2.3 V was obtained by testing three membranes pretreated with 0.1 M RbOH for 24 h: Tokuyama® A210 (Test #5.2), PiperION® (Test #6.1) and Fumasep® FAD-55 (Test #6.2).

Table 12. Current density ($mA \cdot cm^{-2}$) obtained at 2.3 V using different membranes pretreated with 0.1 M RbOH. Test #5.2: Tokuyama® A210 membrane in 0.1 M RbOH for 24 h. Test #6.1: PiperION® membrane in 0.1 M RbOH for 24 h. Test #6.2: Fumasep® FAD-55 membrane in 0.1 M RbOH for 24 h.

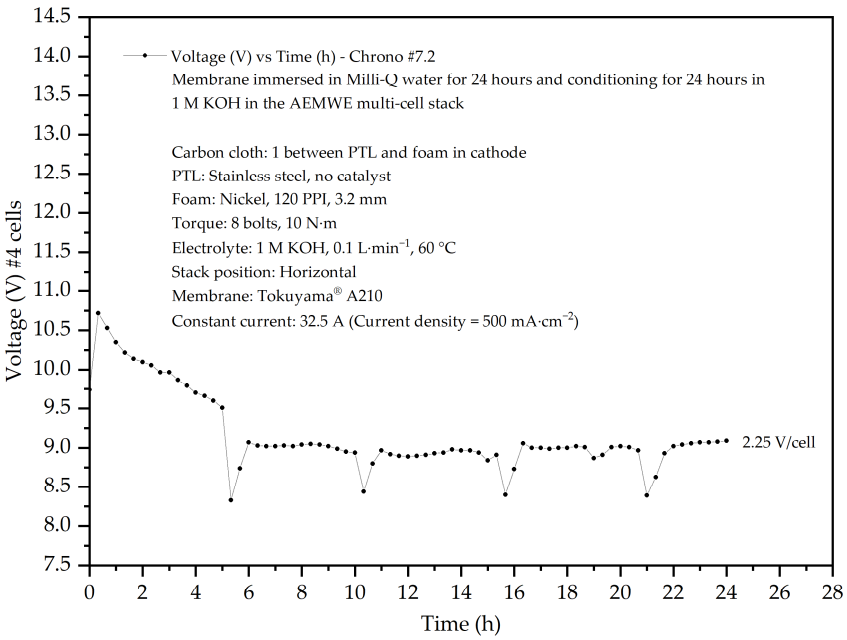
Protocol	Cell Voltage (V)	Current Density ($mA \cdot cm^{-2}$)	SD of Current Density ($mA \cdot cm^{-2}$)
Test #5.2	2.3	329.08	12.16
Test #6.1	2.3	321.66	10.37
Test #6.2	2.3	301.15	26.21

The results show that similar current density values are obtained using RbOH regardless of the type of membrane. RbOH alters the membrane's hydration and ion exchange capacity of all membranes during the pretreatment stage, resulting in similar current densities. The current densities obtained using RbOH in different membranes are lower than

those obtained when KOH is used as the electrolyte (Test #4.1). Therefore, the use of KOH as electrolyte is preferable to RbOH [46,47] and the results from Section 3.1.6. are confirmed (Figure 4g). Complementary, a chronopotentiometry (Figure 5) and ATR-FTIR (Figure 6) analysis are conducted in the following sections to validate these results.

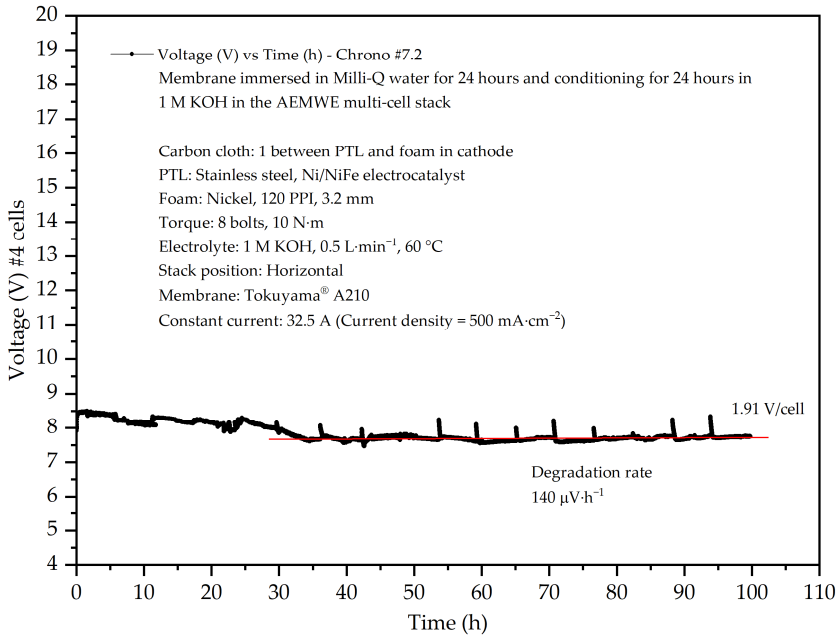


(**a**)



(**b**)

Figure 5. *Cont.*



(**c**)

Figure 5. (**a**) Chrono #0, Chrono #4.1, Chrono #5.2 and Chrono #7.2: Chronopotentiometries obtained from testing for 24 h the AEMWE single-cell stack using Tokuyama® A210 membranes pretreated with different protocols. (**b**) Chrono #7.2: Chronopotentiometry obtained from testing the AEMWE multi-cell stack (4 cells) for 24 h using the Tokuyama® A210 membrane pretreated with the optimal aqueous protocol (Test #7.2). (**c**) Chrono #7.2: Chronopotentiometry obtained from testing the AEMWE multi-cell stack (4 cells) for 100 h using the Tokuyama® A210 membrane pretreated with the optimal aqueous protocol (Test #7.2).

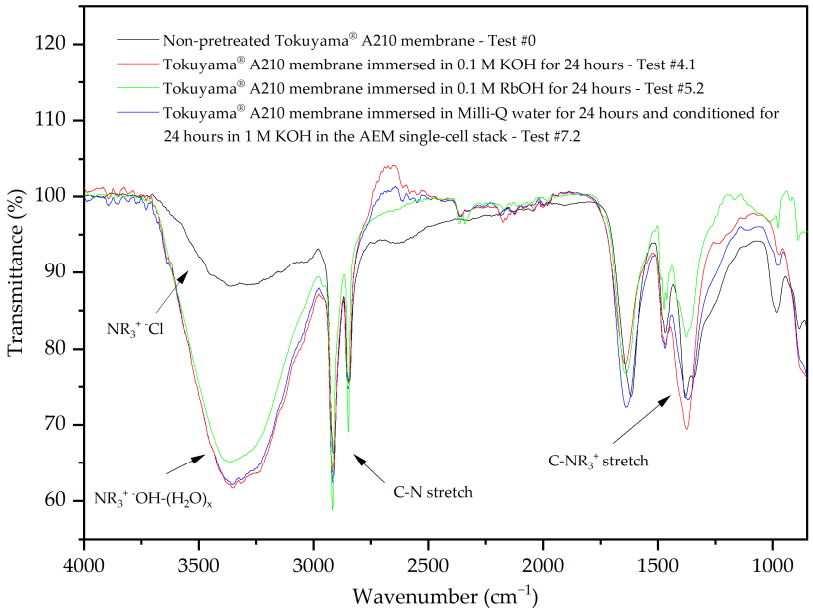


Figure 6. ATR-FTIR spectrum of Tokuyama® A210 membranes pretreated with different protocols (4000–1000 cm^{-1}). Test #0, Test #4.1, Test #5.2 and Test #7.2.

3.1.8. Test #7. Comparison with Zero Reagent-Based Protocols

It has been demonstrated that the Tokuyama® A210 membrane has optimal physico-chemical properties for the pretreatment stage, and that the optimal parameters to carry out

the pretreatment consists of immersing the membranes in 0.1 M KOH for 24 h without cleaning with Milli-Q water (Test #4.1). Next, this result is compared with the conclusions drawn from the authors' previous research [26], which showed that pretreating the membranes for 7 days in Milli-Q water and conditioning it with 1 M KOH in the AEMWE single-cell for 8 h (Test #7.1) allows achieving higher current densities than those observed in the alkaline medium. Additionally, the pretreatment protocol developed in study [26] was optimised. The pretreatment time is reduced to 24 h while the conditioning in the AEMWE single-cell stack is fixed at 24 h (Test #7.2) to assess whether, with the optimal parameters (time and number of immersions) determined for the alkaline medium, the membrane can hydrate properly in less time, without affecting the subsequent ion exchange process (Table 13).

Table 13. Current density ($mA \cdot cm^{-2}$) obtained at 2.3 V using Tokuyama® A210 membranes pretreated with different methodologies (alkaline and aqueous protocols). Test #4.1: Immersion in 0.1 M KOH for 24 h. Test #7.1: Immersion in Milli-Q water for 7 days and conditioned in 1 M KOH for 8 h. Test #7.2: Immersion in Milli-Q water for 24 h and conditioned in 1 M KOH for 24 h.

Protocol	Cell Voltage (V)	Current Density ($mA \cdot cm^{-2}$)	SD of Current Density ($mA \cdot cm^{-2}$)
Test #4.1	2.3	397.77	14.85
Test #7.1	2.3	382.29	1.87
Test #7.2	2.3	391.01	4.11

Figure 4h shows that pretreating the membranes in alkaline and aqueous media leads to comparable current densities. In addition, in the case of the modified aqueous protocol (Test #7.2), current densities comparable to those obtained with the protocol developed in [26] (Test #7.1) have been achieved, despite reducing the pretreatment time from 7 days to 24 h and increasing the conditioning time from 8 h to 24 h (Figure 4h).

3.2. Validation Through Chronopotentiometry Analysis

Several chronopotentiometry tests were performed to further validate the results obtained from the LSV curves over extended operating periods (Figure 5a): Chrono #0 (Chrono refers to the procedure followed to carry out the chronopotentiometry after applying the pretreatment protocols from Table 3): Operate the non-pretreated Tokuyama® A210 membrane (according to Test #0) for 24 h. Chrono #4.1: Operate the Tokuyama® A210 membrane pretreated with 0.1 M KOH (according to Test #4.1) for 24 h to validate the optimal parameters in an alkaline medium. Chrono #5.2: Operate the Tokuyama® A210 membrane pretreated with 0.1 M RbOH (according to Test #5.2) for 24 h to evaluate the effect of inadequate pretreatment parameters on the electrochemical performance of the AEMWE. Chrono #7.2: Operate the Tokuyama® A210 membrane pretreated with Milli-Q water (according to Test #7.2) for 24 h to validate the protocol in aqueous medium. Additionally, Chrono #7.2 was repeated using a four-cell stack to validate the results under multi-cell operating conditions. The stack was operated at 60 °C and a current of 32.5 A (corresponding to 500 $mA \cdot cm^{-2}$) for 24 and 100 h. The 24 h test was conducted without electrocatalysts and with 5 h on/off cycles (Figure 5b), whereas the 100 h test was performed using NiFe as the anode electrocatalyst, Ni as the cathode electrocatalyst, with 8 h on/off cycles and voltage increments of 0.5 V (Figure 5c) to validate the system under long-term operating conditions while maximising hydrogen production through the electrocatalytic effect.

The results shown in Figure 5a demonstrate that the electrochemical behaviour observed in the LSV tests is maintained over time at a constant current of 20 A (314.4 $mA \cdot cm^{-2}$). Pretreat Tokuyama® A210 membranes with 0.1 M KOH for 24 h (Chrono #4.1) and with Milli-Q water for 24 h (Chrono #7.2) enables maintaining a current of 20 A (with a voltage oscillating within the range 2.16–2.20 V), indicating that both procedures yield similar

results. In contrast, when comparing these results with the membrane pretreated using large cation-based electrolyte, RbOH (Chrono #5.2), it is observed that the voltage required to reach the same current is higher (2.3 V), decreasing the Faradaic efficiency of the system by 3.51%. Finally, the result obtained with the non-pretreated membrane (Chrono #0) is the worst of all (2.55 V), significantly reducing the Faradaic efficiency of the system.

Equation (1) allows to calculate the Faradaic efficiency [26]:

$$\eta_{Faraday} = \frac{E_{H_2}}{E_{consumption}} = \frac{M \cdot LHV_{H_2}}{V \cdot z \cdot F} \cdot 100\% \quad (1)$$

where

$\eta_{Faraday}$: Faradaic efficiency (%).
E_{H_2}: Hydrogen energy (Wh).
$E_{consumption}$: Electrical energy consumed by the electrolytic stack (Wh).
M: Molar mass of the substance produced (2 g·mol^{-1} for H_2).
LHV_{H_2}: Hydrogen lower heating value (33.33 Wh·g^{-1}).
V: Cell voltage (V).
z: Valence number of the produced substance (2 for H_2).
F: Faraday constant (96,485.33 C·mol^{-1}).

By applying Equation (1) using the voltage values required to achieve a current density of 314.44 mA·cm^{-2} for Chrono #0 (2.55 V) and Chrono #7.2 (2.16 V), the Faradaic efficiency was calculated, yielding values of 48.77% and 57.57%, respectively. These results demonstrate that the absence of membrane pretreatment results in poorer electrochemical performance. In this case, the system efficiency is reduced by 8.8%. Furthermore, after 4 h of operation under highly controlled laboratory conditions (low current density of 314.4 mA·cm^{-2} and temperature of 25 °C), a short circuit occurred in Chrono #0, causing the cell voltage to rise to 4.10 V (Figure 5a). This further highlights the importance of proper membrane pretreatment, as it compromises system efficiency and reduce the operational lifetime of the electrolysis stack, particularly under high current densities and operating temperatures.

On the other hand, when scaling the system up to four cells and operated at 60 °C with on/off cycles every 5 h, Figure 5b, the membrane pretreated with Milli-Q water for 24 h (Chrono #7.2) reach a current density of 500 mA·cm^{-2} at 2.25 V. This current density value is competitive for an AEMWE in which no precious metal-based electrocatalysts or Ni/Fe formulations are used [26,52–55]. Furthermore, during the 100 h long-term test using Ni/NiFe as the electrocatalyst (Figure 5c), a current density of 500 mA·cm^{-2} was achieved at 1.91 V, together with a low degradation rate of 140 μV·h^{-1} and no evidence of short circuits. Furthermore, the hydrogen produced during this chronopotentiometry was monitored, confirming a purity higher than 99% and demonstrating the excellent separation capability of the pretreated membranes, as well as their low gas crossover.

This experiment demonstrates the excellent chemical and mechanical stability of the membrane pretreated with Milli-Q water for 24 h, thereby confirming the importance of optimising pretreatment parameters as a key step in the overall electrolysis process. Furthermore, the amount of KOH saved by using the aqueous protocol has been estimated with the AEMWE operating at 1.91 V and 500 mA·cm^{-2}. The estimation was based on the KOH savings per 1 kW of power output, comparing the optimised protocols in aqueous and alkaline media. The AEMWE stack used in this study consists of cells with an active area of 63.62 cm^2 and can operate at 1.91 V and 500 mA·cm^{-2} when using the optimised pretreatment parameters in an aqueous medium, delivering a power output of 60.76 W. Therefore, a stack comprising 17 cells is required to achieve a power output of 1 kW. Since each cell incorporates one membrane, and each membrane is pretreated using a 0.1 M KOH solution, this corresponds to a KOH consumption of approximately 5.61 g per membrane.

Consequently, for the 17 membranes required to achieve 1 kW, the aqueous protocol results in estimated savings of approximately 95.37 g of KOH and 17 L of water.

3.3. Validation Through ATR-FTIR

A second validation of the results was carried out using ATR-FTIR. This technique enables the characterisation of the main functional groups of the membrane and helps determine whether the hydration and ion exchange processes have occurred correctly [56,57]. Tokuyama® A210 membranes were analysed by ATR-FTIR after Test #0, Test #4.1, Test #5.2 and Test #7.2. The measurement was carried out using a JASCO® FT/IR-4200 instrument within a wavenumber range of 4000–1000 cm^{-1}.

Tokuyama® A210 membranes have a structure composed of a hydrocarbon backbone linked to ammonium groups with their respective counterions (Cl^-) [13,14]. During the pretreatment stage, the membrane absorbs water, and the counterions are exchanged for OH^- ions. As shown in Figure 6, the bands corresponding to the membranes pretreated with KOH and water (red and blue, respectively) almost completely overlap, indicating that both treatments achieve similar degrees of hydration and ion exchange. However, for the non-pretreated membrane and the membrane pretreated with 0.1 M RbOH for 24 h, there are differences in the spectral regions associated with ammonium and hydroxyl groups (1500–1000 and 4000–3000 cm^{-1}, respectively) [58]. Although the membrane pretreated with 0.1 M RbOH for 24 h exhibited a higher absorption than the non-pretreated membrane, it did not reach the degree of hydration and ion exchange achieved in the membranes pretreated with the most effective protocols (#Test 4.1 and #Test 7.2), as was explained in Sections 3.1.7 and 3.1.8.

3.4. Validation Through Swelling Ratio

Swelling ratio reflects the degree of swelling exhibited by the pretreated membrane. A low swelling ratio is desirable to preserve membrane mechanical stability while maintaining sufficient hydration to facilitate ion transport. According to various studies [59–63], AEMs with optimal electrochemical and mechanical performance typically exhibit swelling ratios in the range of 5–20%. Consequently, the swelling ratios corresponding to the pretreatments which have demonstrated superior electrochemical performance and shorter pretreatment time (Test #4.1, 0.1 M KOH for 24 h and Test #7.2, Milli-Q water for 24 h and conditioning for 24 h with 1 M KOH in the AEMWE single-cell) were measured in order to further validate the results (Table 14).

Table 14. Swelling ratio (SR %), A_{wet} (cm^2) and A_{dry} (cm^2) of Tokuyama® A210 membranes pretreated with the best parameters determined in this study: Test #4.1 (0.1 M KOH for 24 h) and Test #7.2 (Milli-Q water for 24 h and conditioning for 24 h with 1 M KOH in the AEM single-cell).

Pretreatment Protocol	A_{dry} (cm^2)	A_{wet} (cm^2)	SR (%) of Swelling Ratio	SD (%) of Swelling Ratio
Test #4.1	2.78	3.27	17.62	1.28
Test #7.2	3.61	4.16	15.23	3.43

Note. SD represents the standard deviation of swelling ratio (samples number; $n = 4$).

Equation (2) allows to calculate the swelling ratio [60]:

$$SR\ (\%) = \frac{A_{wet} - A_{dry}}{A_{dry}} \cdot 100\% \quad (2)$$

where

SR: Swelling ratio (%).

A_{wet}: Area of a fully hydrated membrane (cm^2).

A_{dry}: Area of a dry membrane (cm^2).

The results obtained show that the swelling ratios achieved by applying the alkaline and aqueous protocols are very similar. This agrees with studies carried out by other researchers [59–63], as the value obtained lies within the 5–20% range. Therefore, both protocols provide comparable results, achieving an adequate degree of membrane hydration without exceeding the swelling ratio that could compromise the mechanical stability and electrochemical performance of AEMs.

3.5. Pretreatment Parameters Used by the Manufacturers

Once the optimal parameters for carrying out the pretreatment in alkaline and aqueous media had been identified and validated, a comparison was made with the parameters recommended by different AEM manufacturers to assess their advantages and disadvantages relative to the approach investigated in this study.

The main conclusions drawn from this study are summarised in Table 15:

Table 15. Comparison of pretreatment protocols for commercial AEMs and improvements proposed in this study [26,39].

Commercial Membranes	Pretreatment Parameters	Disadvantages	Authors' Proposal
Fumasep® FAA-3-50	Rinse the membrane in NaCl solution (e.g., 0.5 M NaCl solution at T = 25 °C for 24 h) to remove any additive from the membrane.	The pretreatment parameters recommended by the manufacturer are intended to convert the membrane into its Cl^--exchanged form, rather than its OH^--form. Therefore, there is ambiguity regarding the optimal parameters for use in an alkaline medium.	The optimal pretreatment parameters are clearly established for both alkaline conditions (0.1 M KOH for 24 h) and aqueous conditions (immersion in Milli-Q water for 24 h, followed by conditioning in the electrolysis stack for a further 24 h).
Fumasep® FAD-55	Rinse the membrane in deionised water (before or after assembling). If additional cleaning is required rinse the membrane in either the application solution or deionised water according to the application requirement.	It is recommended that the membrane be pretreated in the same alkaline solution to be used during electrolysis. However, the optimal parameters are not quantified.	Using the same alkaline solution for both electrolysis and membrane pretreatment does not allow the membrane to achieve an adequate degree of hydration and ion exchange, as these are two distinct electrochemical processes.
PiperION® Versogen's	Place the membrane in an aqueous solution of 0.5 M NaOH or KOH for 1 h at room temperature. After 1 h, replace the solution with fresh 0.5 M NaOH or KOH and allow the membrane to soak for 1 h at room temperature again. After the two soaks, rinse the membrane with DI water (pH ~ 7).	Pretreat the membrane with 0.5 M KOH for 1 h is not an optimal combination of concentration and time, as it does not achieve an adequate degree of membrane hydration and ion exchange. Furthermore, rinsing the membrane with distilled water removes surface ionic charge and is unnecessary unless the pretreatment medium differs from the electrolysis medium.	It uses the optimal KOH concentration (0.1 M) in the alkaline pretreatment protocol and avoids the use of KOH in the aqueous protocol, thereby reducing the environmental impact of the process. Furthermore, it has been demonstrated that rinsing the membrane with deionised water has a detrimental effect on the current density of the system.
Tokuyama® A210	Immerse the membrane in a 0.1 M KOH electrolyte solution for 30 min, repeating the procedure three times using separate containers. Finally, rinse the membrane with deionised water.	Pretreat the membrane with 0.1 M KOH for 30 min, repeated three times, does not provide sufficient time for the membrane to achieve an adequate degree of hydration and ion exchange. As in the previous case, rinsing the membrane with water is not recommended.	Pretreating the membrane for 30 min in three separate 0.1 M KOH solutions does not provide the optimal pretreatment duration (24 h). As in the previous case, rinsing the membrane with deionised water has a detrimental effect on the system's performance.

4. Conclusions

In this study, a multi-parametric investigation was conducted to identify the key factors influencing the pretreatment of anion exchange membranes (AEMs), with the aim of optimising hydrogen production while preventing membrane degradation. Different cleaning protocols, number of immersions, time of immersion, electrolyte concentration,

type of electrolyte and AEMs with different physicochemical properties were compared using LSVs, chronopotentiometries, ATR-FTIR analysis and swelling ratio measurements. The main conclusions are:

1. The pretreatment parameters in the alkaline medium have been optimised to maximise the electrochemical performance of the AEMWE while preventing membrane degradation. It has been found that pretreat AEMs with a specific conductivity > 25 mS·cm^{-1}, ion exchange capacity > 2.0 meq·g^{-1} and a thickness in the range of 20–30 µm using 0.1 M KOH for 24 h is the best option to ensure proper hydration of its internal channels, achieve an optimal ion exchange between the membrane's counterions and the hydroxyl groups in the medium, and prevent degradation of the membrane due to excessive concentrations, prolonged pretreatment times or low membrane thickness.
2. Pretreatment with Milli-Q water for 24 h and conditioning for 24 h with 1 M KOH in the AEM single-cell has proven to be a competitive option compared with the optimised parameters in the alkaline medium. This finding is consistent with previous studies conducted by the authors [26], as sufficient contact time between the AEMs and water allows the internal membrane channels to become adequately hydrated, enabling effective ion exchange during the conditioning stage. Consequently, the overall transport process based on both the vehicular (standard diffusion) and Grotthuss mechanisms is enhanced when employing both optimised methodologies (alkaline and aqueous).
3. The chronopotentiometry results support the findings obtained from the LSV tests in aqueous and alkaline media, demonstrating an 8.81% increase in Faradaic efficiency. In addition, when repeating the test for the membrane pretreated with Milli-Q water for 24 h, scaling the system up to four cells, increasing the temperature to 60 °C and the current to 32.5 A (500 mA·cm^{-2}), it is observed that the AEMWE performance remains stable over 100 h of operation, and competitive current density values are obtained for the applied voltage (1.91 V).
4. The results from the ATR-FTIR tests show that the absorption values obtained in the region between 4000 and 3000 cm^{-1} using the optimal alkaline (0.1 M KOH for 24 h) and aqueous (Milli-Q water for 24 h) protocols are higher than in the case of the non-pretreated membrane and the membrane pretreated with 0.1 M RbOH for 24 h. These findings highlight the importance of establishing the optimal pretreatment parameters for the membranes to ensure an adequate degree of hydration and ion exchange.
5. The swelling ratio values for the optimal protocols in an alkaline and aqueous medium are very similar (17.62 and 15.23%, respectively). Therefore, a good degree of membrane hydration has been achieved, facilitating ion migration through the membrane while maintaining its mechanical stability, with the swelling ratio not exceeding the values reported by other authors (5–20%).

Author Contributions: Conceptualization, M.Á.G. and F.S.; methodology, M.Á.G. and F.S.; software, M.Á.G.; validation, M.Á.G. and F.S.; formal analysis, M.Á.G., F.S., J.M.A. and C.V.; investigation, M.Á.G., F.S., J.M.A. and C.V.; resources, F.S. and J.M.A.; data curation, M.Á.G. and F.S.; writing—original draft preparation, M.Á.G. and F.S.; writing—review and editing, F.S., J.M.A. and C.V.; visualisation, M.Á.G., F.S., J.M.A. and C.V.; supervision, F.S. and J.M.A.; project administration, F.S.; funding acquisition, F.S. and J.M.A. All authors have read and agreed to the published version of the manuscript.

Funding: This research was funded by the Spanish Government, grant (1) Ref: PID2023-148456OB-C4; grant (2) Ref: H2-GIFS Cátedra de la Provincia UHU, and grant (3) EPIT26662026 PdC UHU.

Institutional Review Board Statement: Not applicable.

Informed Consent Statement: Not applicable.

Data Availability Statement: The data presented in this study are available on request from the corresponding authors. The data are not publicly available due to internal agreement between project partnership.

Acknowledgments: Authors would like to thank the materials and disposal offered by research Centre Pro2Tecs, at University of Huelva.

Conflicts of Interest: The authors declare no conflicts of interest.

References

1. Balat, M. Potential importance of hydrogen as a future solution to environmental and transportation problems. *Int. J. Hydrogen Energy* **2008**, *33*, 4013–4029. [CrossRef]
2. Midilli, A.; Ay, M.; Dincer, I.; Rosen, M.A. On hydrogen and hydrogen energy strategies I: Current status and needs. *Renew. Sustain. Energy Rev.* **2005**, *9*, 255–271. [CrossRef]
3. Kapdan, I.K.; Kargi, F. Bio-hydrogen production from waste materials. *Enzym. Microb. Technol.* **2006**, *38*, 569–582. [CrossRef]
4. Andrews, J.; Shabani, B. The role of hydrogen in a global sustainable energy strategy. *Wiley Interdiscip. Rev. Energy Environ.* **2014**, *3*, 474–489. [CrossRef]
5. Miller, H.A.; Bouzek, K.; Hnat, J.; Loos, S.; Bernäcker, C.I.; Weissgärber, T.; Röntzsch, L.; Meier-haack, J. Green hydrogen from anion exchange membrane water electrolysis: A review of recent developments in critical materials and operating conditions. *Sustain. Energy Fuels* **2020**, *4*, 2114–2133. [CrossRef]
6. El-shafie, M. Hydrogen production by water electrolysis technologies: A review. *Results Eng.* **2023**, *20*, 101426. [CrossRef]
7. Gul, E.; Baldinelli, G.; Farooqui, A.; Bartocci, P.; Shamim, T. AEM-electrolyzer based hydrogen integrated renewable energy system optimisation model for distributed communities. *Energy Convers. Manag.* **2023**, *285*, 117025. [CrossRef]
8. Hauch, A.; Küngas, R.; Blennow, P.; Hansen, A.B.; Hansen, J.B.; Mathiesen, B.V.; Mogensen, M.B. Recent advances in solid oxide cell technology for electrolysis. *Science* **2020**, *370*, 6513. [CrossRef] [PubMed]
9. Zakaria, Z.; Kamarudin, S.K. A review of alkaline solid polymer membrane in the application of AEM electrolyzer: Materials and characterization. *Int. J. Energy Res.* **2021**, *45*, 18337–18354. [CrossRef]
10. Henkensmeier, D.; Najibah, M.; Harms, C.; Žitka, J.; Hnát, J.; Bouzek, K. Overview: State-of-the Art Commercial Membranes for Anion Exchange Membrane Water Electrolysis. *J. Electrochem. Energy Convers. Storage* **2021**, *18*, 024001. [CrossRef]
11. Sugawara, Y.; Sankar, S.; Miyanishi, S.; Illathvalappil, R.; Gangadharan, P.K.; Kuroki, H.; Anilkumar, G.M.; Yamaguchi, T. Anion Exchange Membrane Water Electrolyzers: An Overview. *J. Chem. Eng. Jpn.* **2023**, *56*, 2210195. [CrossRef]
12. Santoro, C.; Lavacchi, A.; Mustarelli, P.; DI Noto, V.; Elbaz, L.; Dekel, D.R.; Jaouen, F. What is Next in Anion-Exchange Membrane Water Electrolyzers? Bottlenecks, Benefits, and Future. *ChemSusChem* **2022**, *15*, e202200027. [CrossRef] [PubMed]
13. Ng, W.K.; Wong, W.Y.; Rosli, N.A.H.; Loh, K.S. Commercial Anion Exchange Membranes (AEMs) for Fuel Cell and Water Electrolyzer Applications: Performance, Durability, and Materials Advancement. *Separations* **2023**, *10*, 424. [CrossRef]
14. Wijaya, G.H.; Arum, I.M.; Nam, K.S. Advancements in commercial anion exchange membranes: A review of membrane properties in water electrolysis applications. *Desalin. Water Treat.* **2024**, *320*, 100605. [CrossRef]
15. Hua, D.; Huang, J.; Fabbri, E.; Rafique, M.; Song, B. Development of Anion Exchange Membrane Water Electrolysis and the Associated Challenges: A Review. *ChemElectroChem* **2023**, *10*, e202200999. [CrossRef]
16. CHEN; Chen, T.S.E.; Steve, Y.L.; Lindberg, G.E.; Knight, C.; Voth, G.A. Hydroxide Solvation and Transport in Anion Exchange Membranes. *J. Am. Chem. Soc.* **2016**, *138*, 991–1000. [CrossRef] [PubMed]
17. Foglia, F.; Berrod, Q.; Clancy, A.J.; Smith, K.; Gebel, G.; Sakai, V.G.; Appel, M.; Zanotti, J.-M.; Tyagi, M.; Mahmoudi, N.; et al. Disentangling water, ion and polymer dynamics in an anion exchange membrane. *Nat. Mater.* **2022**, *21*, 555–563. [CrossRef] [PubMed]
18. Yang, L.; Dong, S.; Yang, T.; Liu, J.; Liu, S.; Wang, K.; Wang, E.; Wang, H.; Chou, K.-C.; Hou, X. Membrane Electrode Assembly Design for High-Efficiency Anion Exchange Membrane Water Electrolysis. *Research* **2025**, *8*, 0907. [CrossRef] [PubMed]
19. Hagesteijn, K.F.L.; Jiang, S.; Ladewig, B.P. A review of the synthesis and characterization of anion exchange membranes. *J. Mater. Sci.* **2018**, *53*, 11131–11150. [CrossRef]
20. Espiritu, R.; Golding, B.T.; Scott, K.; Mamlouk, M. Degradation of radiation grafted anion exchange membranes tethered with different amine functional groups via removal of vinylbenzyl trimethylammonium hydroxide. *J. Power Sources* **2018**, *375*, 373–386. [CrossRef]
21. Periasamy, A.P.; Clament Sagaya Selvam, N.; Devadas, B. Addressing degradation and durability challenges in anion exchange membranes for advancing anion exchange membrane water electrolyzers. *Curr. Opin. Chem. Eng.* **2026**, *51*, 101226. [CrossRef]

22. Lindquist, G.A.; Oener, S.Z.; Krivina, R.; Motz, A.R.; Keane, A.; Capuano, C.; Ayers, K.E.; Boettcher, S.W. Performance and Durability of Pure-Water-Fed Anion Exchange Membrane Electrolyzers Using Baseline Materials and Operation. *ACS Appl. Mater. Interfaces* **2021**, *13*, 51917–51924. [CrossRef] [PubMed]
23. Schropp, E.; García Blanco, A.A.; Murcia-lópez, S.; Naumann, G.; Gaderer, M. Multi-criteria optimization of electrode materials for anion exchange membrane water electrolysis regarding energy demand and material criticality. *J. Power Sources* **2024**, *614*, 235031. [CrossRef]
24. Jiang, Z.; Yi, G.; Yao, X.; Ma, Y.; Su, X.; Liu, Q.; Zhang, Q. Durable and highly-efficient anion exchange membrane water electrolysis using poly(biphenyl alkylene) membrane. *Chem. Eng. J.* **2023**, *467*, 143442. [CrossRef]
25. Park, S.B.; Park, J.E.; Na, C.H.O.I.; Geumbi, C.H.O.; Changsoon, Y.H.; Sung, Y.E. Low-Cost and High-Performance Anion-Exchange Membrane Water Electrolysis Stack Using Non-Noble Metal-Based Materials. *ACS Appl. Energy Mater.* **2023**, *6*, 8738–8748. [CrossRef]
26. Rodríguez, M.Á.G.; Delgado, C.; Abiola, A.; Andújar, J.M.; Segura, F. A New Anion Exchange Membranes Pretreatment Protocol for Hydrogen Production by Water Electrolysis. *Energy Technol.* **2025**, *13*, 2500249. [CrossRef]
27. Moreno-González, M.; Mardle, P.; Zhu, S.; Gholamkhass, B.; Jones, S.; Chen, N.; Britton, B.; Holdcroft, S. One year operation of an anion exchange membrane water electrolyzer utilizing Aemion+® membrane: Minimal degradation, low H2 crossover and high efficiency. *J. Power Sources Adv.* **2023**, *19*, 100109. [CrossRef]
28. Lindquist, G.A.; Xu, Q.; Oener, S.Z.; Boettcher, S.W. Membrane Electrolyzers for Impure-Water Splitting. *Joule* **2020**, *4*, 2549–2561. [CrossRef]
29. Yuzer, B.; Selcuk, H.; Chehade, G.; Demir, M.E.; Dincer, I. Evaluation of hydrogen production via electrolysis with ion exchange membranes. *Energy* **2020**, *190*, 116420. [CrossRef]
30. Caire, B.R.; Vandiver, M.A.; Pandey, T.P.; Herring, A.M.; Liberatore, M.W. Accelerated Mechanical Degradation of Anion Exchange Membranes via Hydration Cycling. *J. Electrochem. Soc.* **2016**, *163*, H964–H969. [CrossRef]
31. Lei, J.; Wang, Z.; Zhang, Y.; Ju, M.; Fei, H.; Wang, S.; Fu, C.; Yuan, X.; Fu, Q.; Farid, M.U.; et al. Understanding and resolving the heterogeneous degradation of anion exchange membrane water electrolysis for large-scale hydrogen production. *Carbon Neutrality* **2024**, *3*, 25. [CrossRef]
32. Lyklema, J. Electrokinetics and Related Phenomena. In *Fundamentals of Interface and Colloid Science*; Academic Press: San Diego, CA, USA, 1995; Volume 2, p. 4-1-4-135. [CrossRef]
33. Dukhin, A.S.; Goetz, P.J. Electroacoustic Theory. In *Studies in Interface Science*; Elsevier: Amsterdam, The Netherlands, 2010; Volume 24, pp. 187–237. [CrossRef]
34. Luque DI Salvo, J.; DE Luca, G.; Cipollina, A.; Micale, G. Effect of ion exchange capacity and water uptake on hydroxide transport in PSU-TMA membranes: A DFT and molecular dynamics study. *J. Membr. Sci.* **2020**, *599*, 117837. [CrossRef]
35. Kingsbury, R.S.; Zhu, S.; Flotron, S.; Coronell, O. Microstructure Determines Water and Salt Permeation in Commercial Ion-Exchange Membranes. *ACS Appl. Mater. Interfaces* **2018**, *10*, 39745–39756. [CrossRef] [PubMed]
36. Kingsbury, R.S.; Bruning, K.; Zhu, S.; Flotron, S.; Miller, C.T.; Coronell, O. Influence of Water Uptake, Charge, Manning Parameter, and Contact Angle on Water and Salt Transport in Commercial Ion Exchange Membranes. *Ind. Eng. Chem. Res.* **2019**, *58*, 18663–18674. [CrossRef]
37. Liu, J.; Kang, Z.; Li, D.; Pak, M.; Alia, S.M.; Fujimoto, C.; Bender, G.; Kim, Y.S.; Weber, A.Z. Elucidating the Role of Hydroxide Electrolyte on Anion-Exchange-Membrane Water Electrolyzer Performance. *J. Electrochem. Soc.* **2021**, *168*, 054522. [CrossRef]
38. Amel, A.; Smedley, S.B.; Dekel, D.R.; Hickner, M.A.; Ein-eli, Y. Characterization and Chemical Stability of Anion Exchange Membranes Cross-Linked with Polar Electron-Donating Linkers. *J. Electrochem. Soc.* **2015**, *162*, F1047–F1055. [CrossRef]
39. Fuel Cell Store. Available online: https://www.fuelcellstore.com/ (accessed on 10 November 2025).
40. Yassin, K.; Douglin, J.C.; Rasin, I.G.; Santori, P.G.; Eriksson, B.; Bibent, N.; Jaouen, F.; Brandon, S.; Dekel, D.R. The effect of membrane thickness on AEMFC Performance: An integrated theoretical and experimental study. *Energy Convers. Manag.* **2022**, *270*, 116203. [CrossRef]
41. Rutjens, B.; VON Foerster, K.; Schmid, B.; Weinrich, H.; Sanz, S.; Tempel, H.; Eichel, R.A. Impact of the PiperION Anion Exchange Membrane Thickness on the Performance of a CO_2-to-HCOOH Three-Compartment Electrolyzer. *Ind. Eng. Chem. Res.* **2024**, *63*, 3986–3996. [CrossRef]
42. Silberberg, M.S. *Principles of General Chemistry*, 2nd ed.; McGraw-Hill: Boston, MA, USA, 2007.
43. Haynes, W.M. (Ed.) *CRC Handbook of Chemistry and Physics*, 97th ed.; CRC Press: Boca Raton, FL, USA, 2016.
44. Patnaik, P. *Handbook of Inorganic Chemicals*; McGraw-Hill: Boston, MA, USA, 2002.
45. Mähler, J.; Persson, I. A study of the hydration of the alkali metal ions in aqueous solution. *Inorg. Chem.* **2012**, *51*, 425–438. [CrossRef] [PubMed]
46. Stenina, I.A.; Yaroslavtsev, A.B. Ionic mobility in ion-exchange membranes. *Membranes* **2021**, *11*, 198. [CrossRef] [PubMed]
47. Geise, G.M.; Cassady, H.J.; Paul, D.R.; Logan, B.E.; Hickner, M.A. Specific ion effects on membrane potential and the permselectivity of ion exchange membranes. *Phys. Chem. Chem. Phys.* **2014**, *16*, 21673–21681. [CrossRef] [PubMed]

48. Yaroslavtsev, A.B. Solid electrolytes: Main prospects of research and development. *Russ. Chem. Rev.* **2016**, *85*, 1255–1276. [CrossRef]
49. Peng, J.; Tian, M.; Cantillo, N.M.; Zawodzinski, T. The ion and water transport properties of K+ and Na+ form perfluorosulfonic acid polymer. *Electrochim. Acta.* **2018**, *282*, 544–554. [CrossRef]
50. Shi, S.; Weber, A.Z.; Kusoglu, A. Structure-Transport Relationship of Perfluorosulfonic-Acid Membranes in Different Cationic Forms. *Electrochim. Acta.* **2016**, *220*, 517–528. [CrossRef]
51. Okada, T.; Xie, G.; Gorseth, O.; Kjelstrup, S.; Nakamura, N.; Arimura, T. Ion and water transport characteristics of Nafion membranes as electrolytes. *Electrochim. Acta* **1998**, *43*, 3741–3747. [CrossRef]
52. López-fernández, E.; Gómez-sacedón, C.; Gil-rostra, J.; Espinós, J.P.; Brey, J.J.; González-elipe, A.R.; DE Lucas-consuegra, A.; Yubero, F. Optimization of anion exchange membrane water electrolyzers using ionomer-free electrodes. *Renew. Energy* **2022**, *197*, 1183–1191. [CrossRef]
53. Martinez-séptimo, A.; Gago, A.S.; Gonzalez-huerta, R.d.G.; Najibah, M.; Henkensmeier, D.; Goll, M.; Hosseiny, S. Dissociative electrochemical analysis of materials degradation of an anion exchange membrane electrolyser. *Int. J. Hydrogen Energy* **2024**, *141*, 996–1005. [CrossRef]
54. Ferriday, T.B.; Sampathkumar, S.N.; Middleton, P.H.; Kolhe, M.L.; VAN Herle, J. A Review of Membrane Electrode Assemblies for the Anion Exchange Membrane Water Electrolyser: Perspective on Activity and Stability. *Int. J. Energy Res.* **2024**, *2024*, 7856850. [CrossRef]
55. Dresp, S.; Thanh, T.N.; Klingenhof, M.; Brueckner, S.; Hauke, P.; Strasser, P. Efficient direct seawater electrolysers using selective alkaline NiFe-LDH as OER catalyst in asymmetric electrolyte feeds. *Energy Environ. Sci.* **2020**, *13*, 1725–1729. [CrossRef]
56. Bhargava, R.; Qing, S.; Koenig, J.L. FTIR microspectroscopy of polymeric systems. *Adv. Polym. Sci.* **2003**, *163*, 137–191. [CrossRef]
57. Chércoles Asensio, R.; San Andrés Moya, M.; DE LA Roja, J.M.; Gómez, M. Analytical characterization of polymers used in conservation and restoration by ATR-FTIR spectroscopy. *Anal. Bioanal. Chem.* **2009**, *395*, 2081–2096. [CrossRef] [PubMed]
58. Guerrero-pérez, M.O.; Patience, G.S. Experimental methods in chemical engineering: Fourier transform infrared spectroscopy—FTIR. *Can. J. Chem. Eng.* **2020**, *98*, 25–33. [CrossRef]
59. Xu, W.A.N.; Ziang, L.I.A.O.; Lei, W.A.N.G.; Yiwen, L.I.U.; Peican, K.; Wang, B. Anisotropic anion exchange membranes with extremely high water uptake for water electrolysis and fuel cells. *J. Mater. Chem. A* **2021**, *9*, 23485–23496. [CrossRef]
60. An, E.J.; Sim, G.H.; Yu, S.; Kim, H.G.; An, S.J.; Lee, C.; Kim, M.; Kim, J.H.; Lee, J.H.; Chi, W.S. Cross-linked polysulfone membranes with controllable cross-linkers for anion-exchange membrane water electrolysis. *Eur. Polym. J.* **2024**, *221*, 113543. [CrossRef]
61. Noor Azam, A.M.I.; Ragunathan, T.; Zulkefli, N.N.; Masdar, M.S.; Majlan, E.H.; Mohamad Yunus, S.H.A.M.S.U.L.; Rozan, N.S.; Husaini, T.; Shaffee, S.N.A. Investigation of Performance of Anion Exchange Membrane (AEM) Electrolysis with Different Operating Conditions. *Polymers* **2023**, *15*, 1301. [CrossRef] [PubMed]
62. Khataee, A.; Shirole, A.; Jannasch, P.; Krüger, A.; Cornell, A. Anion exchange membrane water electrolysis using Aemion™ membranes and nickel electrodes. *J. Mater. Chem. A* **2022**, *10*, 16061–16070. [CrossRef]
63. Muhyuddin, M.; Santoro, C.; Osmieri, L.; Ficca, V.C.; Friedman, A.; Yassin, K.; Pagot, G.; Negro, E.; Konovalova, A.; Lindquist, G.; et al. Anion-Exchange-Membrane Electrolysis with Alkali-Free Water Feed. *Chem. Rev.* **2025**, *125*, 6906–6976. [CrossRef] [PubMed]

Disclaimer/Publisher's Note: The statements, opinions and data contained in all publications are solely those of the individual author(s) and contributor(s) and not of MDPI and/or the editor(s). MDPI and/or the editor(s) disclaim responsibility for any injury to people or property resulting from any ideas, methods, instructions or products referred to in the content.